Plant age effects on soil infiltration rate during early plant establishment

Leung, Anthony; Boldrin, David; Liang, Teng; Wu, Z. Y.; Kamchoom, Viroon; Bengough, Anthony

Published in:
Geotechnique

DOI:
10.1680/jgeot.17.T.037

Publication date:
2017

Document Version
Publisher's PDF, also known as Version of record

TECHNICAL NOTE

Plant age effects on soil infiltration rate during early plant establishment

A. K. LEUNG*, D. BOLDRIN*†, T. LIANG*, Z. Y. WU*, V. KAMCHOOM‡ and A. G. BENGOUGH*†

Infiltration rate affects slope stability by determining the rate of water transport to potential failure planes. This note considers the influences of vegetation (grass and willow) establishment and root growth dynamics on infiltration rate, as related to establishing vegetation on bioengineered slopes. Soil columns of silty sand with and without vegetation were tested by constant-head infiltration tests at 2, 4, 6 and 8 weeks after planting. Infiltration rate increased linearly with plant age and below-ground traits including root biomass and root length density. Infiltration rate for willow-rooted soil was an order of magnitude higher than for fallow soil. The plant age effect was more prominent for willow, which grew faster and with thicker roots than the grass. Illustrative seepage analysis suggests that ignoring the plant age effects could underestimate wetting front advancement to greater depths during rainfall, and underestimate suction recovery at shallow depths during internal drainage.

KEYWORDS: partial saturation; permeability; seepage; suction; vegetation; water flow

INTRODUCTION

Soil infiltration rate plays a key role in slope hydrology and stability. It is one of the most important soil parameters that affects prediction of slope failure mechanism, especially when soil–plant interaction in shallow soil is taken into account (Nyambayo & Potts, 2010; Sidle & Bogaard, 2016; Tsiampousi *et al.*, 2017). Plant roots permeated into the soil matrix could modify the soil structure (Scholl *et al.*, 2014; Ng *et al.*, 2016) and hence affect the infiltration rate due to root growth and penetration (Ghestem *et al.*, 2011). Effects of roots on soil infiltrability have often shown contrasting results. Studies that focus on relatively young plants found slowing of infiltration (Gish & Jury, 1983; Leung *et al.*, 2015; Jotisankasa & Sirirattanachat, 2017) presumably due to root occupancy of soil pore space, which blocks water flow paths (Scholl *et al.*, 2014; Ng *et al.*, 2016). In contrast, increased infiltration rate is more often reported in mature plants (van Noordwijk *et al.*, 1991; Mitchell *et al.*, 1995; Ng *et al.*, 2017), and is attributable to the formation of (*a*) root channel related macropores associated with root decay (Ghestem *et al.*, 2011) or (*b*) desiccation cracks upon drying of medium- to high-plasticity clay (Zhan *et al.*, 2007; Jotisankasa & Sirirattanachat, 2017; Song *et al.*, 2017). The existing research often considered plant effects only at one particular plant age. Although limited studies have reported infiltration data at different plant ages (Table 1), the role of root growth dynamics is generally ignored, leaving gaps in the understanding of its effects on infiltration.

This note quantifies effects of plant age on soil infiltration rate and the associated impact on soil hydrology for two contrasting species (herbaceous and woody species). Particular attention is paid to the soil–plant interaction during early plant establishment, which represents a critical period for slope stabilisation using soil bio-engineering methods (Schmidt *et al.*, 2001; Stokes *et al.*, 2014; Sidle & Bogaard, 2016).

METHODS

Selected plant species

Two species were tested, *Salix viminalis tora* (willow) and *Lolium perenne* × *Festuca pratensis* hybrid (Festulolium grass), which represent two plant functional groups that have contrasting root systems. The willow is a fast-growing species, and a common candidate for slope stabilisation in multiple soil bio-engineering projects (Steele *et al.*, 2004; Mickovski *et al.*, 2009; Wu *et al.*, 2014). The grass was bred by the Welsh Plant Breeding Station in the 1970s, and has been recently selected for flood mitigation purposes (Macleod *et al.*, 2013).

Soil type and preparation of soil columns

The soil tested was collected from Bullionfield, The James Hutton Institute, Dundee, UK. It was a silty sand, which comprises 71% sand, 19% silt and 10% clay, and has field capacity of 0·27 g/g. The soil (sieved < 2 mm; optimum water content of 0·18 g/g) was compacted into ten layers in a column of 50 mm dia. and 450 mm high. The targeted dry density was 1400 kg/m^3. At the bottom of each column, a 20 mm thick layer of pea gravel was placed to facilitate drainage during testing.

A pre-germinated seed of grass was sown at 5 mm depth in each soil column. For growing willow, branch cuttings were used – collected in early spring when the willows were dormant. One-third of a 100 mm long branch (12·0 ± 0·1 mm diameter; mean±standard error) was inserted into each soil column. In total, 27 columns were prepared (12 for the grass, 12 for the willow and three for fallow soil as control). All columns were placed in a growing area, where the lighting and temperature were controlled. A data logger (EL-USB-2; Lascar electronics, UK) was used to monitor temperature during day/night cycles (daytime – 16 h of light; 27·3 ± 0·4°C; night – 8 h of dark; 22·2 ± 0·1°C; mean±standard error). Columns were irrigated every 2 days

Manuscript received 31 July 2017; revised manuscript accepted 5 October 2017.
Discussion on this paper is welcomed by the editor.

* Discipline of Civil Engineering, School of Science and Engineering, University of Dundee, Dundee, UK.
† The James Hutton Institute, Invergowrie, Dundee, UK.
‡ Department of Civil and Environmental Engineering, Hong Kong University of Science and Technology, Hong Kong SAR.

Table 1. Studies reporting effects of plant age on infiltration rate or saturated hydraulic conductivity

Species	Soil type and preparation	Plant age	Effect on infiltration rate or saturated conductivity, as compared with fallow soil	Reference
Wheat (*Triticum aestivum*)	Sandy loam and loamy sand soils, repacked to bulk density of 15·2 kN/m^3	Wheat (living plants, single time-point)	Dispersion of solute used to infer degree of bypass flow: < fallow soil for live plants	Gish & Jury (1983)
		Wheat (after 1·5 years' decomposition)	> fallow soil for decomposed plants	
Tulip poplar (*Liriodendron tulipifera*), black gum (*Nyssa sylvatica*) and red maple (*Acer rubrum*)	Field soil – variable deposits from sand to clay	Natural wetland riparian vegetation, indeterminate ages (plant age not a variable)	Evidence of bypass flow from tracer experiments, with bypass flow up to 152 times that of matrix, substantially along dead root channels	Elci & Molz (2009)
White alder (*Alnus incana*)	Poorly graded sand and silty sand, repacked to dry density of 16 kN/m^3	1, 2, 4 and 8 months	Increased with plant age during 2 months of growth, followed by stabilisation at 4 months old and a subsequent decrease at 8 months old	Vergani & Graf (2015)
Scots pine trees (*Pinus sylvestris*)	Field soil – various peaty podzols	Scots pine had grown for 6, 48, 300 or >1000 years on these sites. Single time-point measurements	Increased with forest age by between one and two orders of magnitude	Archer *et al.* (2015)
Vetiver grass (*Chrysopogon zizanioides*)	Low-plasticity silt, repacked to dry density of 13·1 kN/m^3	4–10 months	> fallow soil when root biomass per soil volume is less than ~6 kg/m^3; < fallow soil when root biomass per soil volume is higher than ~6 kg/m^3	Jotisankasa & Sirirattanachat (2017)
	Clayey sand, repacked to dry density of 14 kN/m^3		< fallow soil when root biomass per soil volume is less than ~6 kg/m^3; Similar to fallow soil when root biomass per soil volume is higher than ~6 kg/m^3	

and the amount of water added was used to adjust soil water content to field capacity.

Test procedures

Three replicated soil columns were taken for infiltration testing after growing for 2, 4, 6 and 8 weeks. Before testing, each column was saturated with water for 24 h. A Mariotte bottle was then connected near the top of the column for applying a constant ponding head of 20 mm at the soil surface, while allowing free drainage at the column base. The hydraulic gradient across each soil column was thus controlled at 1·04. The rate of change of water volume in the Mariotte bottle was recorded continuously until a steady-state condition was reached. Steady-state infiltration rate was obtained by dividing the rate of change of water volume by the column sectional area.

To measure the plant traits, root biomass and root length density (RLD), 12 additional columns were prepared in parallel for each plant type (three replications for each plant age). Root samples were excavated and washed from the soil, with extra care taken not to discard finer roots. The measurements of the two plant traits followed the procedures reported in Boldrin *et al.* (2017) and Liang *et al.* (2017).

Statistical analysis

GenStat 17th edition (VSN International) and SigmaPlot13 (Systat Software Inc.) were used for statistical analysis. Significant differences were assessed with one-way Anova (analysis of variance), followed by post hoc Tukey's test. Correlations were tested using Spearman's rank correlation analysis and regression analysis. Results were considered statistically significant when p-value $\leq 0{\cdot}05$.

RESULTS AND DISCUSSION

Figures 1 and 2 highlight contrasting patterns of root growth exhibited by the grass and the willow. It can be seen in Fig. 1 that the root system of grass during the early-stage development (i.e. first 4 weeks) was mainly constituted by very thin roots (i.e. dia. < 0·1 mm), which accounted for about 40% of total root length. Grass roots with a diameter larger than 0·5 mm represent only 3% of total root length. On the contrary, for 2 week old willow (Fig. 2), very thin roots represent less than 20% of total root length. More than 30% of total root length is found in the diameter classes larger than 0·5 mm (i.e. ten-fold higher than in the grass).

The infiltration rate for the vegetated soil was generally faster than for the fallow soil, regardless of plant type and age (Fig. 3, Tables 2 and 3: except for the 2 week old grass). Root growth and penetration therefore might have created sufficient macro-pore space in the soil matrix to enhance infiltration. For both species, infiltration was linearly correlated with plant age (p-value < 0·001). Infiltration rate for the 8 week old willow and grass increased by four and six times, respectively, as compared with the 2 week old plants. Infiltration rate was related to root biomass (Fig. 4(a)) and

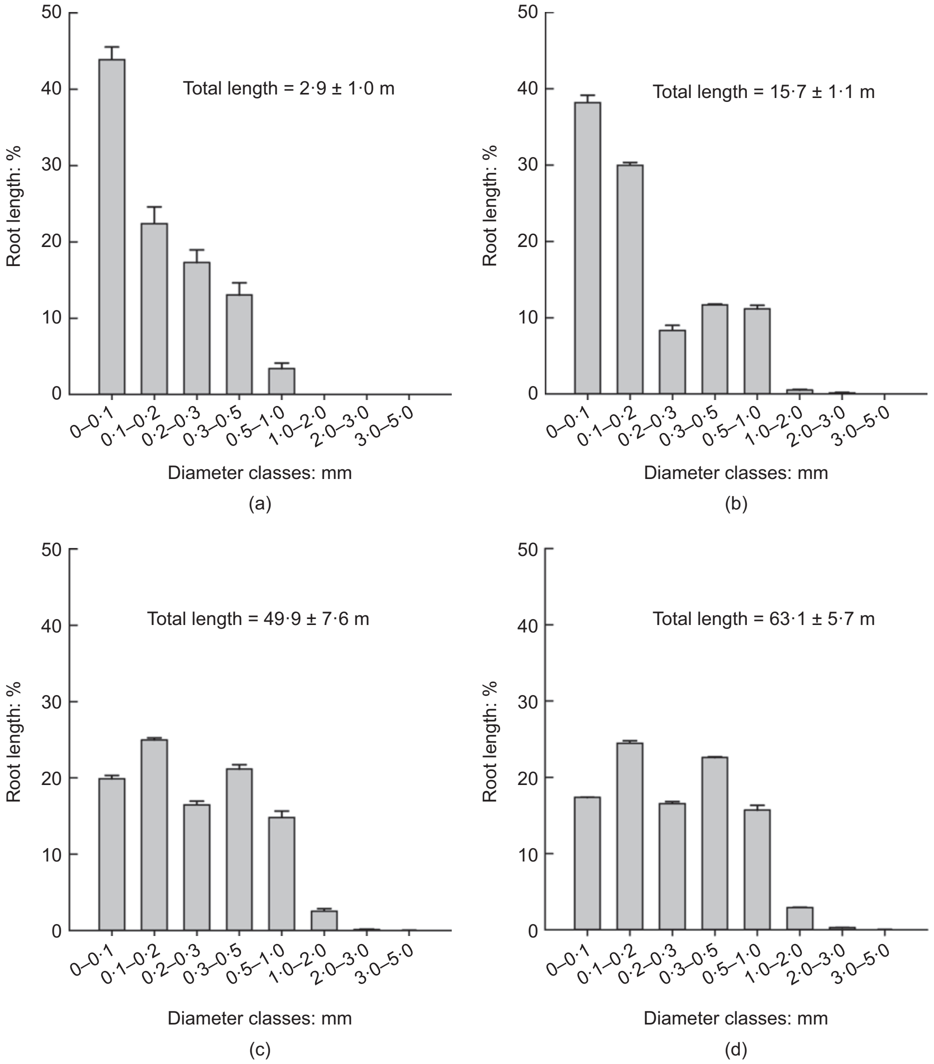

Fig. 1. Percentage of grass root length in each diameter class between <0·1 and 5·0 mm at: (a) 2 weeks; (b) 4 weeks; (c) 6 weeks; (d) 8 weeks. Note that the lower boundary of diameter class is included in the class whereas the upper boundary is not. Values of total root length are given in the graphs. Mean values are reported±standard error of mean (*n* = 3)

RLD (Fig. 4(b)), as these two traits also increased with age (Tables 2 and 3). These relations appear to be species specific. This is because both root biomass and RLD are related to other traits such as root length in each diameter class (Figs 1 and 2), which could at the same time affect these relations.

The faster infiltration rates in willow, as compared with grass at any age, may be due to the faster growth rate of willow and its greater quantity of larger roots (> 0·5 mm) (Figs 1 and 2, and Table 2). Bodner *et al.* (2014) showed that coarser root systems would more prominently increase macro-porosity, while species with dense, finer root systems, such as grass, increase the heterogeneity of soil pore space and increase micro-pore volume. Indeed, very fine roots could permeate and so decrease large micro-pore and fine macro-pore (2·5–500 μm) volume (Scholl *et al.*, 2014). In the present authors' experiments, the very small grass roots may therefore have blocked soil pores and slowed infiltration, whereas larger grass and willow roots may have generated preferential pathways in the soil for water flow.

ENGINEERING IMPLICATIONS

Illustrative transient seepage analysis was conducted to investigate the significance of plant age effects in soil bio-engineering practice. The finite element, Hydrus 1-D (Šimůnek *et al.*, 2013), was used. One-dimensional (1D) seepage in soil was modelled by the Darcy–Richards equation. Two soil hydraulic properties, the soil water retention curve and soil hydraulic conductivity function, are needed to solve the equation. The soil water retention curve of the silty sand was measured by Liang *et al.* (2017) and van Genuchten (1980) model parameters fitted to the data (Table 4). The soil hydraulic conductivity function was estimated using the Muleam–van Genuchten equation (van Genuchten, 1980). The saturated hydraulic conductivity for each case was obtained by dividing the measured steady-state infiltration rate by the hydraulic gradient of 1·04 controlled in all column tests, assuming Darcy's law.

A 1D, 2 m deep soil column, with and without vegetation, was simulated. For vegetated cases, two soil domains were created. Depending on the rooting depth, the top domain represents soil permeated with roots, while the bottom domain represents bare soil. For illustrative purposes, the root growth model proposed by Šimůnek & Suarez (1993) was adopted to estimate the rooting depth at different ages

$$L_{\mathrm{R}}(t) = \frac{L_0}{L_0 + (L_{\mathrm{m}} - L_0)\mathrm{e}^{(-gt)}} L_{\mathrm{m}} \qquad (1)$$

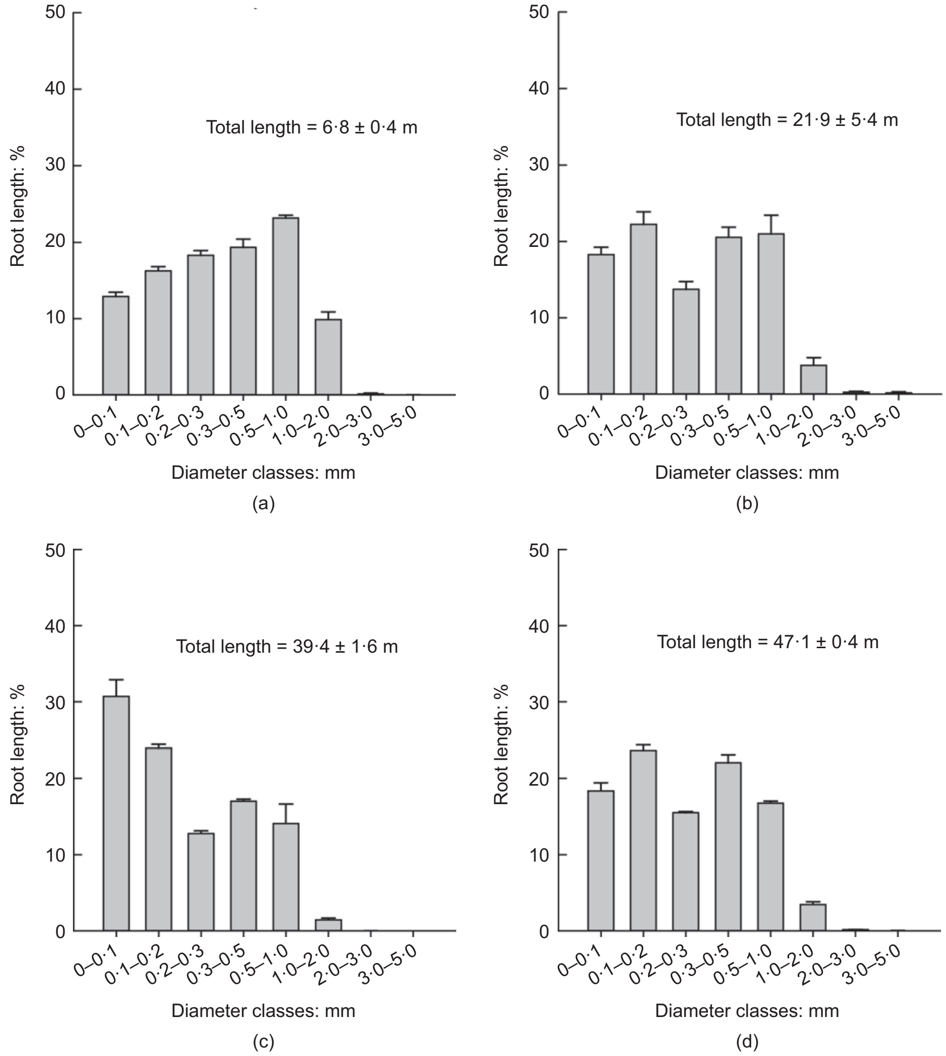

Fig. 2. Percentage of willow root length in each diameter class between <0·1 and 5·0 mm at: (a) 2 weeks; (b) 4 weeks; (c) 6 weeks; (d) 8 weeks. Note that the lower boundary of diameter class is included in the class whereas the upper boundary is not. Values of total root length are given in the graphs. Mean values are reported±standard error of mean ($n = 3$)

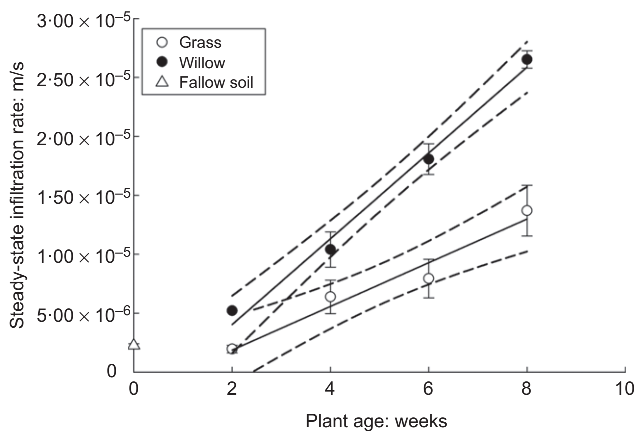

Fig. 3. Relationships between steady-state infiltration rate and the age of grass and willow. Mean values are reported±standard error of mean ($n = 3$). Linear regressions of all data points from all replicates are given in Table 3. Dashed lines represent 95% confidence bands. Spearman's rank correlation analysis between infiltration and plant age of all replications was performed for grass: $r = 0{\cdot}92$ and P-value $< 0{\cdot}001$, and willow: $r = 0{\cdot}97$ and P-value $< 0{\cdot}001$. Triangle on y-axis (open symbol) represents the mean value of infiltration recorded in fallow soil ($2{\cdot}25 \times 10^{-6} \pm 1{\cdot}53$ m/s)

where t is growing period; L_0 is initial rooting depth; L_m is the maximum rooting depth (assumed to be 1·5 m for willow, and 0·5 m for grass); and g is the root growth coefficient. The root growth coefficient is to control the non-linearity of the relationship between rooting depth and growth period. Based on the observed root depth at different plant age (Table 2) and the assumed maximum rooting depth, the root growth coefficient is found to be 0·4 and 0·8 week^{-1} for the willow and the grass, respectively. Hence, rooting depth after 2, 4, 6 and 8 weeks' growth for the willow and the grass are known. At each plant age, the vegetated columns, and a fallow column as control, were subjected to the same rainfall intensity of 10 mm/d for 2 d and then internal drainage for another 8 d. Note that zero plant transpiration and zero canopy rainfall interception was assumed in all analyses (approximating winter conditions for the deciduous willow). All analyses considered a fixed groundwater table at 2 m depth and the initial distribution of suction was hydrostatic.

Figure 5 compares the effects of willow and grass on the distribution of suction (or negative pore-water pressure) after rainfall. Ignoring the plant effects on infiltration underestimated the wetting front advance and, importantly, overestimated the suction preserved at depth during rainfall. Because of increased drainage by plant roots, higher suction was preserved in the surface horizon. Grass roots showed similar trends to willow (Fig. 5(b)) but to a lesser extent, as

Table 2. Summary of measurements (mean±standard error of mean) for both grass and willow

Age: weeks	Infiltration rate: m/s	Root depth: mm	Root biomass: g	Root length density: cm/cm^3
Grass				
2	$1{\cdot}96 \times 10^{-6} \pm 3{\cdot}25 \times 10^{-7}$a	173 ± 0	0·012 ± 0·001a	0·82 ± 0·22a
4	$6{\cdot}39 \times 10^{-6} \pm 1{\cdot}42 \times 10^{-6}$ab	367 ± 1	0·065 ± 0·005b	2·19 ± 0·22a
6	$7{\cdot}93 \times 10^{-6} \pm 1{\cdot}64 \times 10^{-6}$ab	450 ± 2	0·338 ± 0·010c	5·64 ± 0·86b
8	$1{\cdot}37 \times 10^{-5} \pm 2{\cdot}16 \times 10^{-6}$b	450 ± 3	0·461 ± 0·025c	7·14 ± 0·64b
Willow				
2	$5{\cdot}21 \times 10^{-6} \pm 2{\cdot}34 \times 10^{-9}$a	256 ± 16	0·075 ± 0·005a	2·42 ± 0·80a
4	$1{\cdot}04 \times 10^{-5} \pm 1{\cdot}50 \times 10^{-6}$b	450 ± 0	0·154 ± 0·014b	3·00 ± 0·67ab
6	$1{\cdot}81 \times 10^{-5} \pm 1{\cdot}30 \times 10^{-6}$c	450 ± 0	0·352 ± 0·022c	4·46 ± 0·18ab
8	$2{\cdot}65 \times 10^{-5} \pm 7{\cdot}35 \times 10^{-7}$d	450 ± 0	0·552 ± 0·035d	5·33 ± 0·05b

Note: Letters indicate significant differences as tested using one-way Anova followed by post hoc Tukey's test (root biomass data for both species and infiltration rate data for willow were square root transformed in statistical analysis). Note that root depth was constrained to a maximum of 450 mm, due to column dimensions

Table 3. Summary of the fitting coefficients (m and y_0±standard error) and adjusted coefficient of determination (R^2) for the linear relationships ($f = y_0 + m \times x$) given in Figs 3 and 4

Relationship	Figure	m	y_0	Adj. R^2
Grass				
Infiltration rate against age	3	$1{\cdot}85 \times 10^{-6} \pm 3{\cdot}28 \times 10^{-7}$	$-1{\cdot}83 \times 10^{-6} \pm 1{\cdot}83 \times 10^{-6}$	0·76
Infiltration rate against root biomass	4(a)	$2{\cdot}06 \times 10^{-5} \pm 6{\cdot}42 \times 10^{-6}$	$2{\cdot}99 \times 10^{-6} \pm 1{\cdot}85 \times 10^{-6}$	0·76
Infiltration rate against RLD	4(b)	$1{\cdot}53 \times 10^{-6} \pm 4{\cdot}26 \times 10^{-7}$	$1{\cdot}44 \times 10^{-6} \pm 2{\cdot}00 \times 10^{-6}$	0·80
Willow				
Infiltration rate against age	3	$3{\cdot}64 \times 10^{-6} \pm 2{\cdot}75 \times 10^{-7}$	$-3{\cdot}24 \times 10^{-6} \pm 1{\cdot}57 \times 10^{-6}$	0·95
Infiltration rate against root biomass	4(b)	$4{\cdot}34 \times 10^{-5} \pm 2{\cdot}43 \times 10^{-6}$	$2{\cdot}76 \times 10^{-6} \pm 8{\cdot}23 \times 10^{-7}$	0·99
Infiltration rate against RLD	4(b)	$6{\cdot}93 \times 10^{-6} \pm 6{\cdot}26 \times 10^{-7}$	$-1{\cdot}13 \times 10^{-5} \pm 2{\cdot}49 \times 10^{-6}$	0·98

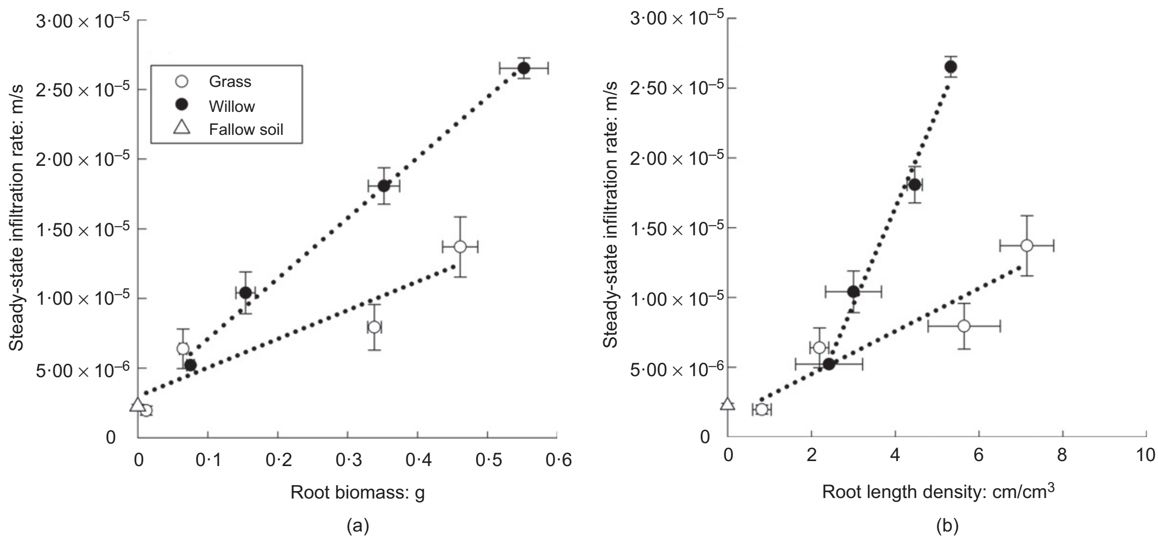

Fig. 4. (a) Relationships between steady-state infiltration and root biomass for grass and willow. (b) Relationships between steady-state infiltration and root length density for grass and willow. Mean values are reported±standard error of mean ($n = 3$). Dotted lines represent the trends in the relationships between infiltration and root traits (Table 3). Triangle on y-axis (open symbol) represents the mean value of infiltration recorded in fallow soil ($2{\cdot}25 \times 10^{-6} \pm 1{\cdot}53$ m/s)

they influenced saturated conductivity less. The results imply that, as far as deep-seated failure (i.e. below rooting depth) is concerned, it may be unconservative simply to use the fallow soil saturated conductivity in slope stability calculations (i.e. to assume that root growth has a negligible effect during early tree establishment).

Willow had larger effects on suction redistribution than grass after 8 days of drainage (Fig. 6). Root growth-induced increase in saturated conductivity caused greater suction recovery in surface horizons. This means that the ability of plants to create soil water deficit is underestimated when the plant age effects are ignored. Although greater suction recovery is beneficial to slope stability, for other applications such as landfill cover design, ignoring root age effects could degrade the accuracy of soil water balance calculations.

SUMMARY AND CONCLUSIONS

This study quantified the effects of roots and their growth for two distinct plant functional types (grass and willow) on water infiltration rate during early plant establishment. Root growth induced an increase in infiltration rate by up

Table 4. Summary of input parameters for seepage analysis

Treatment	Rooting depth: m	Hydraulic properties for van Genuchten (1980) model*				
		α: kPa^{-1}	n	θ_r	θ_s	k_s: m/s
Fallow	N/A	0·15	1·43	0·170	0·383	$2{\cdot}16 \times 10^{-6}$
2 week willow	0·256					$5{\cdot}03 \times 10^{-6}$
4 week willow	0·450					$9{\cdot}95 \times 10^{-6}$
6 week willow	0·630					$1{\cdot}74 \times 10^{-5}$
8 week willow	0·800					$2{\cdot}56 \times 10^{-5}$
2 week grass	0·172					$2{\cdot}16 \times 10^{-6}$
4 week grass	0·367					$6{\cdot}13 \times 10^{-6}$
6 week grass	0·450					$7{\cdot}64 \times 10^{-6}$
8 week grass	0·500					$1{\cdot}32 \times 10^{-5}$

*Note: The fitting parameters, α, n, θ_r and θ_s are obtained from Liang *et al.* (2017).

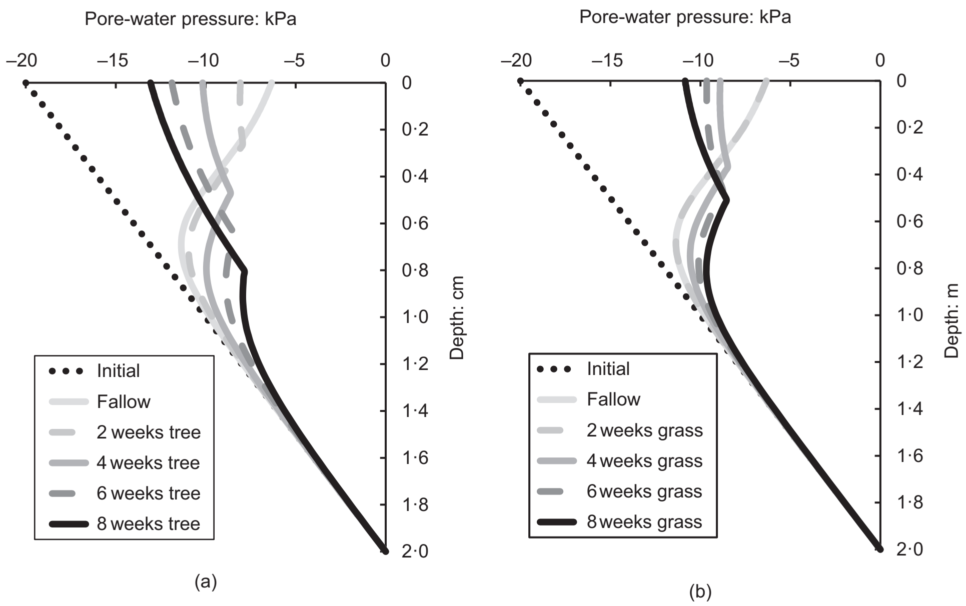

Fig. 5. Simulated pore-water pressure profiles at different plant ages after 2 days of rainfall when soil is vegetated with (a) the willow and (b) the grass

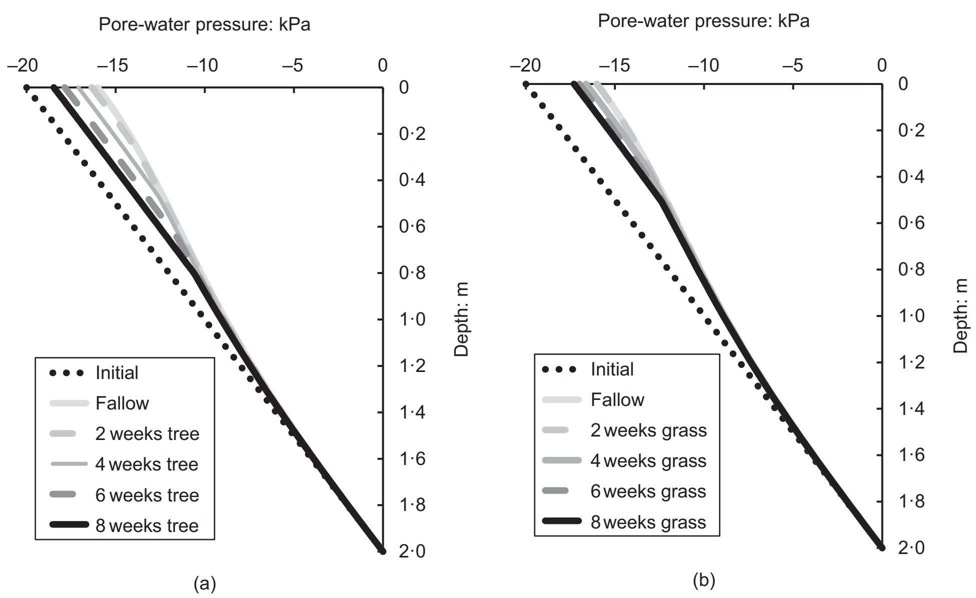

Fig. 6. Simulated pore-water pressure profiles at different plant ages after 8 days of internal drainage when soil is vegetated with (a) the willow and (b) the grass

to an order of magnitude, compared to fallow soil. The root age effect was more prominent for willow, which grew faster and had thicker roots than grass. A positive correlation was identified between infiltration rate and plant age. Below-ground plant traits including root biomass and root length density could explain the infiltration rate for individual species. Illustrative seepage analysis suggests that ignoring the plant root and its age effects on soil hydraulic conductivity could underestimate wetting front advancement to depth during rainfall, and underestimate suction recovery at shallow depths during internal drainage. Compared to grass roots, willow roots introduced more significant changes in soil hydrology at this early growth stage.

ACKNOWLEDGEMENTS

Funding is acknowledged from EU FP 7 Marie Curie Career Integration grant (project BioEPIC slope; AKL and DB); the Engineering and Physical Sciences Research Council (EPSRC) grant EP/M019713/1 (AGB and TL); the Chinese Scholarship Council (ZW) and the Hong Kong/Scotland Partners of Post-Doctoral Research grant (S-HKUST601/15; VK). The James Hutton Institute receives funding from the Scottish government. Thanks to Professor Mike Humphreys (IBERS, Aberystwyth University) for providing grass seed for this study.

NOTATION

g	root growth coefficient
k_s	hydraulic conductivity at saturation
L_m	maximum rooting depth
L_R	rooting depth at time t
L_0	initial rooting depth
m, y_0	fitting coefficients
t	growing period
α, n, θ_r, θ_s	fitting parameters

REFERENCES

Archer, N. A. L., Otten, W., Schmidt, S., Bengough, A. G., Shah, N. & Bonell, M. (2015). Rainfall infiltration and soil hydrological characteristics below ancient forest, planted forest and grassland in a temperate northern climate. *Ecohydrol.* **9**, No. 4, 585–600.

Bodner, G., Leitner, D. & Kaul, H. P. (2014). Coarse and fine root plants affect pore size distributions differently. *Plant Soil* **380**, No. 1, 133–151.

Boldrin, D., Leung, A. K. & Bengough, A. G. (2017). Correlating hydrologic reinforcement of vegetated soil with plant traits during establishment of woody perennials. *Plant Soil* **416**, No. 1–2, 437–451.

Elci, A. & Molz, F. J. (2009). Identification of lateral macropore flow in a forested riparian wetland through numerical simulation of a subsurface tracer experiment. *Water Air Soil Pollut.* **197**, No. 1–4, 149–164.

Ghestem, M., Sidle, R. C. & Stokes, A. (2011). The influence of plant root systems on subsurface flow: implications for slope stability. *Bio Science* **61**, No. 11, 869–879.

Gish, T. J. & Jury, W. A. (1983). Effect of plant roots and root channels on solute transport. *Trans. Am. Soc. Agric. Biol. Engng* **26**, No. 2, 440–444.

Jotisankasa, A. & Sirirattanachat, T. (2017). Effects of grass roots on soil-water retention curve and permeability function. *Can. Geotech. J* **54**, No. 11, 1612–1622.

Leung, A. K., Garg, A., Coo, J. L., Ng, C. W. W. & Hau, B. C. H. (2015). Effects of roots of *Cynodon dactylon* and *Schefflera heptaphylla* on water infiltration rate and soil hydraulic conductivity. *Hydrol. Process.* **29**, No. 15, 3342–3354.

Liang, T., Bengough, A. G., Knappett, J. A., Muir Wood, D., Loades, K. W., Hallett, P. D., Boldrin, D., Leung, A. K. & Meijer, G. J. (2017). Scaling of the reinforcement of soil slopes by living plants in a geotechnical centrifuge. *Ecol. Engng*, https://doi.org/10.1018/j.ecoleng.2017.06.067.

Macleod, C. J. A., Humphreys, M. W., Whalley, W. R., Turner, L., Binley, A., Watts, C. W., Skot, L., Joynes, A., Hawkins, S., King, I. P., O'Donovan, S. & Haygarth, P. M. (2013). A novel grass hybrid to reduce flood generation in temperate regions. *Sci. Rep.* **3**, article 1683.

Mickovski, S. B., Hallett, P. D., Bransby, M. F., Davies, M. C. R., Sonnenberg, R. & Bengough, A. G. (2009). Mechanical reinforcement of soil by willow roots: impacts of root properties and root failure mechanism. *Soil Sci. Soc. Am. J.* **73**, No. 4, 1276–1285.

Mitchell, A. R., Ellsworth, T. R. & Meek, B. D. (1995). Effect of root systems on preferential flow in swelling soil. *Communs Soil Sci. Plant Analysis* **26**, No. 15–16, 2655–2666.

Ng, C. W. W., Ni, J. J., Leung, A. K. & Wang, Z. J. (2016). A new and simple water retention model for root-permeated soils. *Géotechnique Lett.* **6**, No. 1, 106–111, https://doi.org.10.1680/jgele.15.00187.

Ng, C. W. W., Ni, J. J., Leung, A. K., Zhou, C. & Wang, Z. J. (2017). Effects of planting density on tree growth and induced suction. *Géotechnique* **66**, No. 9, 711–724, https://doi.org/10.1680/jgeot.15.P.196.

Nyambayo, V. & Potts, D. M. (2010). Numerical simulation of evapotranspiration using a root water uptake model. *Comput. Geotech.* **37**, No. 1–2, 175–186.

Schmidt, K. M., Roering, J. J., Stock, J. D., Dietrich, W. E., Montgomery, D. R. & Schaub, T. (2001). The variability of root cohesion as an influence on shallow landslide susceptibility in the Oregon Coast Range. *Can. Geotech. J.* **38**, No. 5, 995–1024.

Scholl, P., Leitner, D., Kammerer, G., Lioskandl, W., Kaul, H. P. & Bodner, G. (2014). Root induced changes of effective 1D hydraulic properties in a soil column. *Plant Soil* **381**, No. 1–2, 193–213.

Sidle, R. C. & Bogaard, T. A. (2016). Dynamic earth system and ecological controls of rainfall-initiated landslides. *Earth-Sci. Rev.* **159**, 275–291.

Šimůnek, J. & Suarez, D. L. (1993). Modelling of carbon dioxide transport and production in soil: 1. Model development. *Water Resources Res.* **29**, No. 2, 487–497.

Šimůnek, J., Sejna, H., Saito, M. & van Genuchten, M. T. (2013). *The HYDRUS-1D software package for simulating the one-dimensional movement of water, heat and multiple solutes in variably-saturated media*. Riverside, CA, USA: Department of Environmental Sciences, University of California Riverside.

Song, L., Li, J. H., Zhou, T. & Fredlund, D. G. (2017). Experimental study on unsaturated hydraulic properties of vegetated soil. *Ecol. Engng* **103**, Part A, 207–216.

Steele, D., MacNeil, D., Barker, D. & McMahon, W. (2004). *The use of live willow piles for stabilising highway slopes*, TRL Report No. 619, 685. Crowthorne, UK: Transport Research Laboratory.

Stokes, A., Douglas, G. B., Fourcaud, T., Giadrossich, F., Gillies, C., Hubble, T., Kim, J. H., Loades, K. W., Mao, Z., McIvor, I. R., Mickovski, S. B., Mitchell, S., Osman, N., Phillips, C., Poesen, J., Polster, D., Preti, F., Raymond, P., Rey, F., Schwarz, M. & Walker, L. R. (2014). Ecological mitigation of hillslope instability: ten key issues facing researchers and practitioners. *Plant Soil* **377**, No. 1–2, 1–23.

Tsiampousi, A., Zdravkovic, L. & Potts, D. M. (2017). Numerical study of the effects of soil–atmosphere interaction on the stability and serviceability of cut slopes in London clay. *Can. Geotech. J.* **54**, No. 3, 405–418.

van Genuchten, M. T. (1980). Closed-form equation for predicting the hydraulic conductivity of unsaturated soils. *Soil Sci. Soc. Am. J.* **44**, No. 5, 892–898.

van Noordwijk, M., Widianto, H. M. & Hairah, K. (1991). Old tree root channels in acid soils in the humid tropics: Important for crop root penetration, water infiltration and nitrogen management. *Dev. Plant Soil Sci.* **134**, No. 1, 37–44.

Vergani, C. & Graf, F. (2015). Soil permeability, aggregate stability and root growth: a pot experiment from a soil bioengineering perspective. *Ecohydrol.* **9**, No. 5, 830–842.

Wu, T., Kokesh, C., Trenner, B. & Fox, P. (2014). Use of live poles for stabilisation of a shallow slope failure. *J. Geotech. Geoenviron. Engng* **140**, No. 10, paper 05014001.

Zhan, T. L. T., Ng, C. W. W. & Fredlund, F. G. (2007). Field study of rainfall infiltration into a grassed unsaturated expansive soil slope. *Can. Geotech. J.* **44**, No. 4, 392–408.